A self-consistent model to describe the temperature dependence of the bulk modulus, thermal expansion and molar volume compatible with 3rd generation CALPHAD databases

Guillaume Deffrennes, Benoit Oudot

A self-consistent model to describe the temperature dependence of the bulk modulus, thermal expansion and molar volume compatible with 3rd generation CALPHAD databases

Guillaume Deffrennes[a], Benoit Oudot[a]

[a] CEA, DAM, VALDUC, F-21120 Is-sur-Tille, France

Corresponding author: Dr. Benoit Oudot

Postal address: CEA, DAM, VALDUC, F-21120 Is-sur-Tille, France

Tel.: +33 380234000

Fax: +33 380235217

e-mail : benoit.oudot@cea.fr

e-mail (1st author): guillaume.deffrennes@cnrs.fr

Keywords: Modeling, Volume, Thermal expansion, Bulk modulus, CALPHAD, Sn

Abstract

Variation of volume with temperature is a significant engineering consideration for numerous applications. In addition, the molar volume is a central property along with the bulk modulus in the scope of developing high pressure Gibbs energy multi-component databases. In this work, a semi-empirical model is proposed to describe the bulk modulus, thermal expansion coefficient and molar volume at atmospheric pressure. It is built based on a multi-frequency Einstein-Grüneisen model. The present methodology has several advantages over the use of polynomial functions. First of all, a self-consistent description of the molar volume and related properties together with heat capacity is achieved. This is an interesting feature in the scope of performing consistent assessments of diverse data in joint optimizations. Second, this description is directly compatible with the 3rd generation CALPHAD framework, as some parameters are shared in common. Therefore, it can be used to develop multi-component molar volume databases. Third, the model is built on physical considerations, enabling to perform reliable extrapolations outside the range of available data. Finally, the proposed description is valid down to 0K, allowing a direct integration of *ab initio* calculations. The above mentioned features are highlighted in the assessment of α-Sn and β-Sn, for which a critical review of the literature data is provided, as well as of solid CaO. The obtained results suggest that the proposed model can be applied successfully to a large variety of elements and compounds, as it can notably account for unusual features such as a negative thermal expansion coefficient at low temperature.

1. Introduction

Variation of the molar volume of materials with temperature is a significant engineering consideration for multi-material assemblies and composites. Indeed, thermal expansion mismatch may cause detrimental interfacial stress in those structures. This problematic is encountered in numerous engineering applications, such as in biomaterials [1], cement-based composites [2], thermal coatings [3], automotive assemblies [4], electronic packaging [5], and many others. It should be emphasized that contractions under cryogenic temperatures are also a source of concern for high-end applications, such as in aerospace with cryogenic space telescopes [6]. Furthermore, volume changes during solidification, or during phase transformations in general, is an important consideration as it may cause various defects [7]. To answer those problematics, a precise knowledge of the thermal expansion coefficient of a wide variety of materials at atmospheric pressure is requested. This information can be implemented in CALPHAD databases, which are considered a cornerstone of the Integrated Computational Materials Engineering (ICME) approach and of the Materials Genome Initiative (MGI) [8–10]. Besides, to include a description of molar volume in thermodynamic databases would allow the calculations of volume fractions versus temperature.

In addition, in a theoretical point of view, thermal expansion is an important property as it is directly linked to lattice vibrations in crystals, the anharmonicity of the interatomic potential, and thermal defects [11,12]. As such, thermal expansion is closely related to other thermodynamic and thermophysical properties such as heat capacity and elastic constants.

Therefore, when those intrinsic relationships are captured in a model, the overall consistency of the diverse available data can be assessed in joint optimizations.

Finally, the modeling of molar volume and its related properties is the key to build high pressure Gibbs energy thermodynamic databases. Indeed, by definition, molar volume is the pressure derivative of the Gibbs energy. Therefore, the following expression can be obtained:

$$\Delta G_m(T,P) = \Delta G(T,P_0) + \int_{P_0}^{P} V_m(T,P')dP' \quad (1)$$

with ΔG_m the molar Gibbs energy of a phase relative to a given reference state, P_0 the atmospheric pressure, and V_m the molar volume. Current Gibbs energy CALPHAD databases were designed for applications at atmospheric pressure, and a description of the molar volume of the phases is therefore rarely included. Yet, motivated by applications in geophysics or in high pressure processing of metal and alloys, the extension of those databases towards high pressure using Eq. (1) attracted attention from several research groups in recent years [13–25]. To achieve this purpose, the most common practice is to describe the molar volume in two distinctive steps. First of all, the molar volume and its related properties are modeled as a function of temperature at atmospheric pressure. Then, in a second step, the obtained descriptions are injected into a selected isothermal equation of state that account for the effect of pressure. This approach is somewhat consistent with the fact that the description of the Gibbs energy is separated according to Eq. (1) into an atmospheric pressure part, and a high pressure part. In this study, only the first step will be then covered. Nevertheless, it has to be

pointed out here that so far, the extension of Gibbs energy databases towards high pressure has been considered unsuccessful, because it has been leading to unphysical extrapolations in the high pressure range [26]. A solution to this problem is to build Helmholtz energy databases instead. Indeed, the underlying models have an explicit physical meaning, and satisfying extrapolations can be obtained in the T-P space. However, it is then challenging to account for the effect of composition in thermodynamic functions [27]. Therefore, to the best of our knowledge, Helmholtz energy approaches are currently mostly limited to describing unaries or isoplethal sections of higher-order systems, and cannot benefit from the major strength of the CALPHAD method which lies in the treatment of complex multi-component systems. Besides, in Helmholtz energy databases, molar volume is a characteristic variable instead of pressure, and is therefore not explicitly described, but can only be obtained numerically by derivation. For those reasons, the assessment of molar volume in Helmholtz energy databases is then not considered in the present study, and reviews [26,28] on the matter can be found elsewhere.

In conclusion, there is a significant interest in implementing descriptions of the molar volume at atmospheric pressure and its related properties in Gibbs energy CALPHAD databases. Those thermophysical properties are intrinsically related to the heat capacity, and this relationship is captured by the Grüneisen parameter, which can be expressed as [29]:

$$\gamma = \frac{\alpha K_T V_m}{C_V} \quad (2)$$

with γ the Grüneisen parameter, α the volumetric thermal expansion coefficient (CTE), K_T the isothermal bulk modulus, and C_V the isochoric heat capacity. So far, the thermal expansion coefficient and the bulk modulus at atmospheric pressure were assessed separately using polynomial functions of temperature. Such models are not based on any physical considerations, and are typically not valid below room temperature. This framework is consistent with the 2nd generation of CALPHAD databases, in which heat capacity is also described in a similar fashion [30]. In this work, a semi-empirical model is proposed to achieve a self-consistent description of the molar volume and its related properties at atmospheric pressure together with heat capacity. Its parameters have an explicit physical meaning, enabling to extend the validity of descriptions down to 0K and to make reasonable extrapolations outside of the range of available data. The proposed description is directly compatible with 3rd generation CALPHAD databases [31–36] in both form and content, as it shares the same aim and some parameters in common.

Hereafter, the theoretical framework of the proposed descriptions will first be presented. In a second place, the proposed model will be put to the test in the modeling of α-Sn and β-Sn, for which a critical review of the available data will be provided, and of solid CaO. In this process, several benefits of the model will be demonstrated, a summary of which will be given in the conclusion.

2. Theoretical framework

The most common expressions that are currently used to describe the coefficient of thermal expansion at atmospheric pressure are polynomial functions of temperature [12–14,16–18,20,25,28,30,37,38]. They adopt the following general form:

$$\alpha(T) = \sum_i \alpha_i T^{p_i} \quad (3)$$

with α_i the fitting parameters, and p_i an integer. It is reminded that α is the volumetric, and not linear, thermal expansion coefficient.

Descriptions of the thermal expansion coefficient obtained using Eq. (3) usually require using 3 to 4 fitting parameters, and are typically not valid below room temperature. Besides, as the parameters do not have an explicit physical meaning, extrapolations outside the range of the available data are uncertain. It is emphasized that the mathematical formalism to describe the isobaric heat capacity in 2nd generation CALPHAD databases is the same as Eq. (3). This similarity stems from the fact that heat capacity and thermal expansion are intrinsically related. Therefore, as suggested by Hallstedt at al. [30], similar models and approximations can be made to describe either of those properties. Finally, it is noted that a few other phenomenological models were used in the literature as an alternative to Eq. (3) [15,22]. They share the same empirical nature, but are designed so that the thermal expansion would tend to a limited value at very high temperature.

In contrast with empirical models such as Eq. (3), some attempts to describe thermal expansion using theoretical models were made in the literature, as reviewed by Wang and Reeber [11]. However, a precise representation of experimental data is hardly obtained with those approaches.

Finally, semi-empirical models provide expressions in which parameters have an explicit physical significance and can be determined by least-square fitting of experimental data [11]. Such models are often built based on formulations of the Grüneisen parameter [11,39] by making different hypothesis, assumptions, and choices of expressions. In the present work, this approach will be followed, aiming at finding a model offering a compromise between its physical soundness, its capacity to achieve a precise representation of experimental data, and its ease of implementation in thermodynamic databases. An explicit expression for thermal expansion will be determined as a by-product from the description of the other properties linked through the Grüneisen parameter. Eq. (2) is therefore re-arranged as follows:

$$\alpha = \frac{\gamma}{V_m}\frac{C_V}{K_T} \tag{4}$$

First of all, let us focus on the ratio of the Grüneisen parameter over the volume. An approximation commonly used for solids is that this ratio is temperature independent above the Debye temperature [29,40]. A justification of this approximation can be obtained considering the variation with temperature of the other parameters involved in Eq. (4). Indeed, above the Debye temperature, the isochoric heat capacity tends towards *3nR* in the quasi-harmonic approximation, and there is experimental evidences that the product αK_T tends to

become temperature independent as well [29,40]. Then in this work, the hypothesis that the ratio of the Grüneisen parameter over the volume is temperature independent is considered to hold at any temperature, leading to:

$$\frac{\gamma}{V_m} = \frac{\gamma_0}{V_{m_0}} \tag{5}$$

with γ_0 and V_{m_0} the Grüneisen parameter and the molar volume at a given reference temperature, respectively. The fact that this approximation is extended below the Debye temperature in this work might result in an inaccurate description in this domain. It will be highlighted later on that it does not seem to be the case as satisfying results were obtained in the low temperature range for the materials investigated in this study.

Then, let us focus on the description of the isochoric heat capacity. In this work, the general framework provided at the 1995 Ringberg meeting [41], and later implemented in the so-called 3rd generation CALPHAD databases [31–36], is adopted. The isochoric heat capacity will therefore be modeled as the sum of its various physical contributions.

Regarding the harmonic contributions, it was recommended at the 1995 Ringberg meeting to either use a Debye or an Einstein model [41]. In practice, the Einstein model was adopted in 3rd generation CALPHAD databases [31–36] due to its ease of implementation, although it is not expected to provide the most accurate descriptions at very low temperatures [41]. To obtain a more satisfying fit, multi-frequency Einstein models were used in some later studies [32,33,35]. In short, instead of considering that all atoms oscillate with a unique averaged

frequency, the phase is modeled using a few distinct atom populations each vibrating at their own frequency. It was notably highlighted by Deffrennes et al. [35] that in the case of CaO, the approximate fit obtained at low temperature using a single Einstein function was detrimental to the fit at higher temperature, and affected the modeling of the non-harmonic contributions as well. Then, the following multi-frequency Einstein expression is therefore adopted in this work:

$$C_V^{ha}(T) = 3R\sum_i a_i \left(\frac{\theta_i}{T}\right)^2 \frac{\exp\left(\frac{\theta_i}{T}\right)}{\left(\exp\left(\frac{\theta_i}{T}\right)-1\right)^2} \quad (6)$$

with C_V^{ha} the harmonic contributions to the isochoric heat capacity, R the gas constant, θ_i the Einstein temperature for the ith mode of vibration, and a_i the corresponding pre-factor constrained so that the sum all a_i is equal to the phase stoichiometry. It is important to stress out that in CALPHAD databases, Eq. (6) is applied to the modeling of the isobaric, and not isochoric, heat capacity. Nonetheless, both of those thermodynamic properties are equivalent at low temperatures, which is actually the domain where the fitting of the thermodynamic parameters is made. Therefore, the parameters of Eq. (6) can either be taken directly from 3rd generation thermodynamic databases, or be adjusted in a joint optimization of the isobaric heat capacity data and of the thermophysical properties considered in this work. This is a central feature of the proposed description, as it enables to perform consistent modeling of diverse data, to ensure a direct compatibility with 3rd generation CALPHAD databases, and to use a reduced number of parameters overall. It will be highlighted later on that a direct usage

of the Einstein functions already modeled in the thermodynamic databases can lead to very satisfying results for the properties investigated in this work.

Then, regarding anharmonic contributions to the isochoric heat capacity, they can be most simply expressed as a linear function of the temperature [29,42]. In addition, it was suggested by Chase et al. [41] that a "bT^2" term might also be needed to describe higher-order anharmonic effects. Besides, the electronic contributions are generally expressed in the framework of the Helmholtz free energy databases as a linear function of temperature [27,29,43,44]. At very high temperatures, *ab initio* calculations highlight that the rise of the electronic heat capacity with temperature becomes steeper [45,46], and it was suggested by Chase et al. [41] to use a quadratic term to account for this deviation. Therefore, in this work, anharmonic and electronic contributions to the isochoric heat capacity are both accounted for without distinction using the following expression:

$$C_V^{anh-el}(T) = AT + BT^2 \quad (7)$$

It is important to note that the A and B parameters from Eq. (7) are not the same as the thermodynamic parameters that share the same form and meaning used in 3rd generation CALPHAD databases to model the isobaric heat capacity.

Finally, the last expression needed to achieve a description of the thermal expansion coefficient using Eq. (4) is the one of the isothermal bulk modulus. In previous work [13,14,17,18,25], the compressibility was most commonly expressed as follows:

$$\chi_T(T) = \sum_i \chi_i T^{p_i} \tag{8}$$

with χ_T the isothermal compressibility, χ_i the fitting parameters, and p_i a positive integer for the corresponding powers of T. To obtain the expression for the bulk modulus from Eq. (8) is straightforward, as it is the inverse of compressibility:

$$K_T = \frac{1}{\chi_T} \tag{9}$$

An interesting equation to describe the temperature dependency of elastic constants was provided by Varshni [47]. The author proposed an expression based on physical considerations and on the Einstein model. Following Ledbetter [48], we write the expression from Varshni [47] as follows:

$$K_T(T) = K_{T_0} - \frac{s}{\exp\left(\frac{\theta}{T}\right) - 1} \tag{10}$$

with K_{T_0} the bulk modulus at the reference temperature, s a positive material-dependent parameter, and θ the characteristic Einstein temperature. However, it can be argued that Eq. (10) present two downsides. First, at very high temperature, the bulk modulus might become negative. Second, as discussed by Varshni [47], this expression is not expected to give very precise results at low temperatures due to the limitations inherent to the Einstein model. To address both theses downsides, the following expression is adopted in this work:

$$\chi_T(T) = \chi_{T_0} + C \sum_i \frac{a_i}{\exp\left(\frac{\theta_i}{T}\right) - 1} \quad (11)$$

with χ_{T_0} the compressibility at the reference temperature, C a material-dependent parameter, and θ_i and a_i the very same Einstein temperature for the ith mode of vibration and corresponding pre-factor as in Eq. (6). The bulk modulus can be obtained from Eq. (11) by its definition given in Eq. (9). The relation proposed by Varshni [47] and given in Eq. (10) was inverted so that the bulk modulus cannot reach negative values anymore at very high temperatures. It can be shown that very similar fit can be obtained for the bulk modulus nonetheless using either Eq. (10) or (11). Indeed, differences will only appear at very high temperatures, as Eq. (11) will smoothly tend to 0. Besides, it can also be shown that Eq. (11) can give almost identical results as Eq. (8) that is currently being used in 2nd generation databases, except in the low temperature range that is not taken into account in the latter model. Finally, a multi-frequency Einstein model was used in Eq. (11) to be consistent with the description adopted for the heat capacity in Eq. (6), and with recent work on the 3rd generation CALPHAD databases [32,33,35]. This is expected to improve the precision of the fit at low temperature.

At last, injecting the descriptions proposed in Eq. (5), (6), (7) and (11) into the formulation of the Grüneisen parameter presented Eq. (4), an expression for thermal expansion can be obtained as follows:

$$\alpha(T) = \frac{3R}{V_{m_0}} \sum_i \gamma_{i_0} a_i \left(\left(\frac{\theta_i}{T}\right)^2 \frac{e^{\frac{\theta_i}{T}}}{\left(e^{\frac{\theta_i}{T}} - 1\right)^2} + AT + BT^2 \right) \left(\chi_{T_0} + \frac{C}{e^{\frac{\theta_i}{T}} - 1} \right) \quad (12)$$

with γ_{i_0} the Grüneisen parameter at the reference temperature associated with the ith Einstein mode of vibration.

Eq. (12) leaves us with an important issue that needs to be addressed. The molar volume at atmospheric pressure can be obtained from the thermal expansion coefficient according to:

$$V_m(T) = V_{m_0} \exp\left(\int_{T_0}^{T} \alpha(T) dT \right) \quad (13)$$

Yet, there is no explicit expression for the primitive of the ratio of anharmonic and electronic contributions to the isochoric heat capacity with the bulk modulus, that is:

$$\frac{C_V^{anh-el}}{K_T}(T) = (AT + BT^2) \sum_i a_i \left(\chi_{T_0} + \frac{C}{e^{\frac{\theta_i}{T}} - 1} \right) \quad (14)$$

In this work, to obtain an explicit expression for the molar volume was considered to be an important feature so that this central property can be calculated straightforwardly. However, it is actually a significant constraint, as it requires that the expressions for all properties linked through the Grüneisen parameter are compatible with each other, in the sense that an explicit primitive of the thermal expansion coefficient can be obtained from their combination. To achieve this purpose, the temperature dependent part of the compressibility from which the

issue arise in Eq. (14) is approximated by its first-order Laurent series expansion at infinite temperature, which gives:

$$\frac{1}{e^{\frac{\theta}{T}}-1} \sim \frac{T}{\theta} - \frac{1}{2} \tag{15}$$

The original expression in Eq. (15) and its first-order Laurent expansion are compared in Fig. 1(a). Obviously, below the material's Einstein temperature, this approximation gives poor results. However, it is important to underline the error will only apply to the temperature dependent part of the compressibility, which is very small in this temperature range. In addition, in this relatively low temperature range, the anharmonic and electronic contributions for the isochoric heat capacity can be reasonably considered to be negligible compared to their harmonic counterpart, and the error will be then reduced even further. In order to illustrate those considerations, the error induced by the proposed approximation on the overall thermal expansion coefficient of β-Sn, which modeling will be discussed at a later stage, is presented in Fig. 1(b). Although the relative error when the ratio of the temperature over the averaged Einstein temperature is lower than 0.1 seems impactful, the numbers are somewhat misleading, as in this temperature range the thermal expansion coefficient is not significantly different from 0. For instance, when the ratio of the temperature over the averaged Einstein temperature equals 0.01, a maximal relative error of 2.6% is obtained, yet the corresponding absolute error of 4.14 10^{-10} K^{-1} represents only 2 10^{-9} % of the thermal expansion coefficient at room temperature. At higher temperature, the relative error decreases rapidly and is no more that 0.04 % at the averaged Einstein temperature. All things considered, the

approximation made in Eq. (15) has a negligible impact on the calculated thermal expansion of β-Sn, and it is reasonable to consider that the result will be the same regardless of the material. Therefore, Eq. (15) is considered to be a reasonable approximation, and the following final expression is obtained for the thermal expansion coefficient:

$$\alpha(T) = \frac{3R}{V_{m_0}} \sum_i \gamma_{i_0} a_i \left(\left(\frac{\theta_i}{T}\right)^2 \frac{e^{\frac{\theta_i}{T}}}{\left(e^{\frac{\theta_i}{T}} - 1\right)^2} \left(\chi_{T_0} + \frac{C}{e^{\frac{\theta_i}{T}} - 1} \right) + \left((AT + BT^2) \left(\chi_{T_0} + C \left(\frac{T}{\theta_i} - \frac{1}{2} \right) \right) \right) \right) \tag{16}$$

In Eq. (16), the first part in the summation is the ratio of the harmonic contributions to the heat capacity with the original expression of the bulk modulus, and the second part is the one including the ratio of the anharmonic and electronic contributions to the heat capacity with the approximated expression for the bulk modulus.

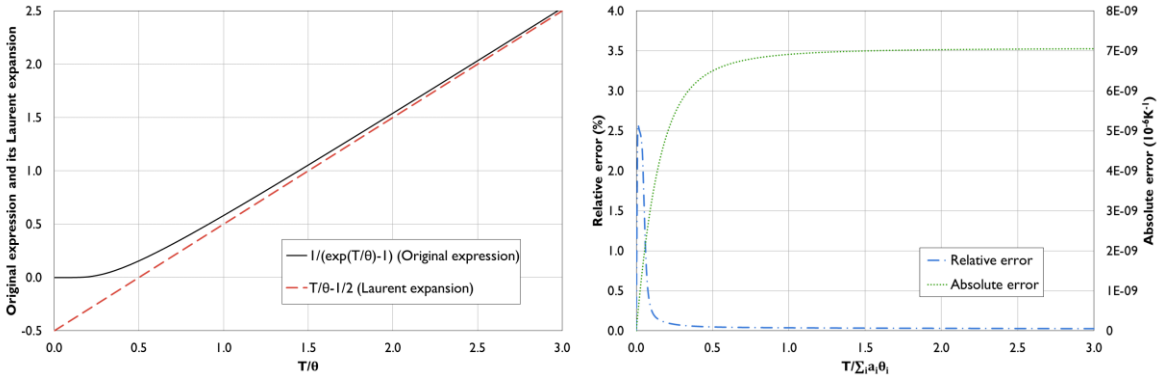

(a) (b)

Fig. 1. (a) Comparison between the original expression that is included in the description of the bulk modulus and its first-order Laurent series expansion at infinite temperature and (b) illustration taking the case of β-Sn that the resulting error on the thermal expansion coefficient is negligible

The integration of Eq. (16), that is needed to obtain the molar volume according to Eq. (13), gives the following explicit expression:

$$\int \alpha(T) = \frac{3R}{V_{m_0}} \sum_i \gamma_{i_0} a_i \left(\theta_i \left(\frac{\chi_{T_0}}{e^{\frac{\theta_i}{T}} - 1} + \frac{C}{2\left(e^{\frac{\theta_i}{T}} - 1\right)^2} \right) + \left(\frac{AT^2}{2}\left(\chi_{T_0} - \frac{C}{2}\right) + \frac{T^3}{3}\left(\frac{AC}{\theta_i} + B\chi_{T_0} - \frac{BC}{2}\right) + \frac{BCT^4}{4\theta_i} \right) \right) \quad (17)$$

It is important to stress out that, despite appearances, Eq. (17) can be viewed as a simplification compared to the polynomial expression that were commonly used presented in Eq. (3). Indeed, the only parameters that are directly related to the description of the thermal expansion coefficient are the Grüneisen parameters γ_{i_0} associated with each Einstein mode of vibration, and when appropriate the A and B parameters to account for anharmonic and electronic contributions. Regarding the other parameters, the Einstein contributions can be either taken directly from the description of the isobaric heat capacity in 3rd generation CALPHAD databases, or adjusted in a joint optimization with the isothermal bulk modulus

and the isochoric or isobaric heat capacity. Then, the only parameters left, that are V_0 and C, are respectively obtained from molar volume and isothermal bulk modulus data. In the case where only scarce or debated thermal expansion data are available, a single Grüneisen parameter common for all Einstein mode of vibrations may be taken. For instance, a description of the thermal expansion of β-Sn valid down to 0 K will be provided later on using only 2 parameters directly related to the modeling of this property.

The proposed model shares some similarities with the expressions proposed by Wang and Reeber [11], and more recently by Zhang et al. [39]. Indeed, semi-empirical models were proposed in both studies based on the definition of the Grüneisen parameter. Regarding the work of Wang and Reeber [11], a multi-frequency Einstein model was used by the authors in the description of the heat capacity, similarly as in this work. Differences from the present model mainly stems from the treatment of non-harmonic contributions and of the bulk modulus, as well as the hypothesis made in the formulation of the Grüneisen parameter. The ratio $\gamma_i a_i / K_T V_m$ was notably treated by Wang and Reeber [11] as an overall parameter that was optimized for each of the i^{th} Einstein frequencies, whereas each term was treated independently in this work. As a result, it can be argued that in the present work it is more straightforward to identify the meaning of each parameters and whether reasonable values were obtained or not. Plus, the treatment of the temperature dependence of the bulk modulus can be directly included in the analysis. Regarding the work of Zhang et al. [39], the authors used a Debye model to describe the heat capacity. Therefore, it is argued that the description proposed in this work benefit from a greater ease of implementation in thermodynamic

databases, and a direct compatibility with the 3rd generation CALPHAD framework. Besides, an explicit description of the isothermal bulk modulus and of the molar volume was obtained in this work.

As final notes of this section, it is first highlighted that the molar volume obtained using Eq. (13) and Eq. (17) does not include any magnetic contribution. It is suggested that for magnetic materials, this contribution may be treated in a separate term [12,37] as based on the work of Guillermet [13,49]. Besides, the proposed descriptions do not account for the pressure dependence of the considered thermophysical properties, and is excepted to be valid up to roughly 1 GPa [30]. Last but not least, the present study focuses on the modeling of stoichiometric end-members, which are the building blocks for modeling solution phases. The composition dependence of the molar volume and bulk modulus can be accounted for in a typical CALPHAD fashion, by a rule of mixtures between end-members, plus an excess contribution described by a Redlich-Kister polynomial that includes interaction parameters. This general approach is for instance presented in [50]. In practice however, there have been a limited number of attempts to model the molar volume of solution phases. This is due to a lack of data on volumes of mixing [30], and to the fact that the molar volume has not been considered so far as an essential part of thermodynamic databases [38]. A method to determine the molar volume of metastable or non-stable end-members was discussed by Hallstedt [38], and new insights on this matter within the framework of the 3rd generation of CALPHAD thermodynamic databases were recently provided by He et al. [36]. The molar volume of various solid solutions were assessed by Hallstedt [38] and Xiong et al. [50] along

the room temperature isotherm. Both the molar volume and the isothermal compressibility of several binary solution phases in the Al-Cu-Mg system were modeled by Huang et al. [51] using temperature independent interaction parameters. The experimental study from Schmitz et al. [52] suggests that the excess volume of the Al-Li liquid phase is temperature dependent. To account for this temperature dependence may not be straightforward within the model proposed in this work, as 3rd generation CALPHAD models to describe solution phases are still under development [34,36]. In the 2nd generation of CALPHAD thermodynamic databases, interaction parameters are described as linear functions of T to account for the temperature dependence of the excess Gibbs energy. However, as discussed by Dinsdale et al. [34], this approach lead to a non-configurational entropy that is different from 0 at 0 K, and therefore to a loss of physical realism. In the present case, it will similarly lead to a non-zero thermal expansion coefficient at 0 K. To be consistent with the aspirations of 3rd generation databases, it was suggested by Dinsdale et al. [34] to account for the temperature dependence of the excess properties using parameters expressing the variation of the Einstein temperature with respect to composition. To apply this approach to the present model is an interesting perspective, although it is noted that to do so, the treatment proposed by Dinsdale et al. [34] has to be extended to the case where multiple Einstein frequencies are used. It is concluded that the extension of the proposed framework to the modeling of solution phases is an open question that is closely linked to the development of the 3rd generation of CALPHAD thermodynamic databases.

3. Results and discussion

3.1 Modeling procedure

In the present study, the thermal expansion coefficient is described in a self-consistent way with the heat capacity through the Grüneisen parameter. As discussed in the previous section, a multi-frequency Einstein model was selected as the basis to describe the thermal expansion coefficient and the bulk modulus. This notably ensures a direct compatibility of the present model with the ones used in 3rd generation CALPHAD databases to describe the isobaric heat capacity. To further highlight both features, the parameters of the Einstein functions that will be used for each phase considered in this work will be directly taken from recent CALPHAD assessments of their heat capacity.

In the following section, assessments of α-Sn, β-Sn, and solid CaO are proposed. For each of these phases, the modeling procedure was the following. First, for each Einstein mode of vibration, the Einstein temperature and its corresponding pre-factor were taken from recent thermodynamic CALPHAD assessments after their robustness was carefully checked. Then, the bulk modulus of the considered phase was modeled using Eq. (11) and (9). Finally, the thermal expansion coefficient and the molar volume were assessed based on Eq. (16), and Eq. (13) and (17) respectively. The parameters accounting for the anharmonic and electronic contributions as defined by Eq. (7) were only used if a satisfying fit could not be obtained without them.

The parameters optimization and the calculations presented in this work were performed using the Thermo-Calc software package [53]. Based on the model implemented in the software by Lu et al. [18], the compressibility, integrated thermal expansion coefficient, and molar volume at the reference temperature can be entered using the parameters "VK", "VA" and "V0" respectively. A demonstration macro file that can be used to set-up the present model in Thermo-Calc is given in a Mendeley Data repository [54]. Indeed, due to Fortran programming restrictions, only "simple-terms" can be used when entering functions in the software [55]. Therefore, the model has to be entered piece by piece, which may be cumbersome without having a starting example.

A tabulation of all the data reviewed and calculated in this section can be found along with the thermodynamic database files in an open access Mendeley Data repository [54].

3.2 Assessment of α-Sn

The α-Sn phase is stable up to 286.35 K at atmospheric pressure [33], and is commonly referred to as grey tin. α-Sn crystallizes in a diamond-like face-centered structure (space group $Fd\overline{3}m$, Pearson symbol *cF*8).

The isobaric heat capacity of α-Sn was recently assessed by Khvan et al. [33] using a multi-Einstein model including two modes of vibration. A comparison of the authors' results with literature data is provided in the Mendeley Data repository [54] associated with this work. Only the relatively low temperature range that is relevant to assess the parameters of the multi-Einstein model was considered in the analysis. A more detailed review of each

experimental dataset was given by Khvan et al. [33]. The description proposed by the authors was found to be robust up to 100 K, and more uncertain above this temperature due to the lack of reliable experimental data, but still satisfying. Therefore, the parameters relative to the Einstein contributions proposed by Khvan et al. [33] are accepted in the present modeling.

The experimental data relative to the molar volume [56–59], thermal expansion coefficient [60], and bulk modulus [61–64] of α-Sn are reviewed in Table 1. In the treatment of the data from Price et al. [64], the adiabatic bulk modulus was calculated from the elastic constants reported by the authors using the Voigt-Reuss-Hill approximation [65]. This method of calculation was notably discussed by Chung [66], and the corresponding equations are presented in the appendix. The adiabatic bulk modulus data given directly or indirectly in the various studies reviewed in Table 1 [61–64] were transformed into isothermal bulk modulus data according to the following expression [67]:

$$K_T = \frac{K_S}{1 + \frac{V_m \alpha^2 K_S T}{C_P}} \tag{18}$$

with K_S the adiabatic bulk modulus and T the absolute temperature. To obtain some of the data required for the conversion, a preliminary fit of the molar volume and thermal expansion coefficient was performed. Besides, the isobaric heat capacity data were taken from the description proposed by Khvan et al. [33].

Table 1 - Experimental data relative to the molar volume, thermal expansion coefficient, and bulk modulus of α-Sn at atmospheric pressure

Ref	Data	Method	T-range (K)	Relative uncertainty
[56] Bij19	Molar volume	X-ray diffraction	291.15	N/A
[57] Bro50			298.15	0.02%
[58] The54			143 - 295	N/A
[59] Oeh15			298.15	N/A
[60] Nov60	Thermal expansion	Quartz dilatometer	24 - 217	N/A
[61] Red60	Adiabatic bulk modulus	Piezo-electric oscillator method	273.15	N/A
[62-63] Pri69&Buc71		Neutron inelastic scattering	90	2%
[63] Buc71		Raman scattering	77	N/A
[64] Pri71	Adiabatic elastic constants	Spectrometric method	300	N/A

First of all, the data relative to the bulk modulus [61–64] of α-Sn and the description obtained using Eq. (11) and (9) are presented in Fig. 2. The measurement from Reddy et al. [61] is a clear outliner, as further suggested by *ab initio* studies [68,69], and was therefore not taken into account in the modeling. A very satisfying representation of all the other available experimental data [62–64] was obtained.

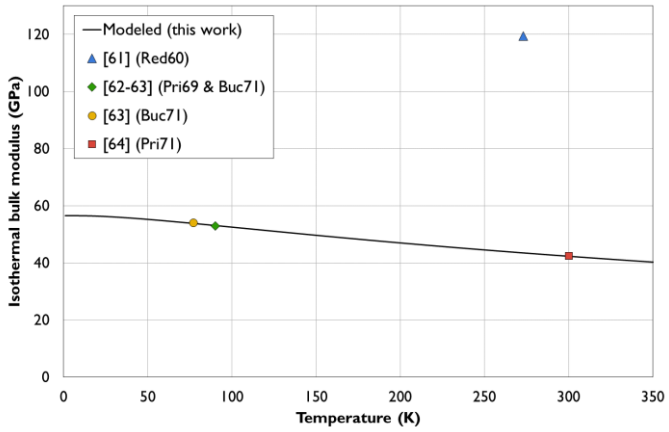

Fig. 2. Experimental and assessed isothermal bulk modulus of α-Sn

α-Sn exhibits a negative thermal expansion coefficient at very low temperature [60], and it is therefore an interesting material to test the proposed model with. This behavior is common for phases crystallizing in diamond-type structures [60], and was notably recently discussed by Ishida [70]. Results from the modeling are presented along with the measurements from Novikova [60] in Fig. 3. The model closely reproduces experimental data, including below 50 K where the thermal expansion coefficient is reported to be negative. A practical explanation of this unusual behavior is that negative Grüneisen parameters are obtained for high-frequency vibrational modes [70], a feature that can be captured by the present model. It is noted that this close agreement obtained using the modes of vibration of the multi-Einstein model proposed by Khvan et al. [33] further support the validity of both descriptions.

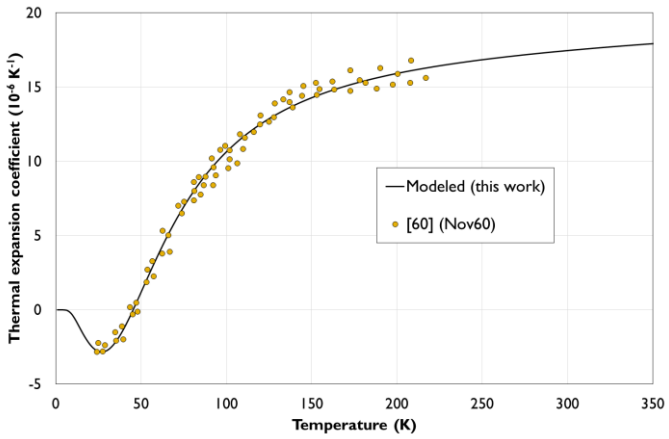

Fig. 3. Experimental and assessed thermal expansion of α-Sn

Finally, the assessment of the molar volume of α-Sn is presented along with the available literature data [56–59] in Fig. 4. A maximal deviation of roughly 1.5% is observed among the available experimental data. In the present modeling, only the dataset from Thewlis [58] was considered in the fit. There are two reasons behind this choice. First, it is the only dataset that also provides information on the thermal expansion coefficient. Second, it is in an acceptable agreement with the data from Brownlee [57] that is the accepted value in the Wyckoff compilation [71]. A satisfying agreement between the thermal expansion coefficient reported by Novikova [60] and the one measured by Thewlis [58] is observed.

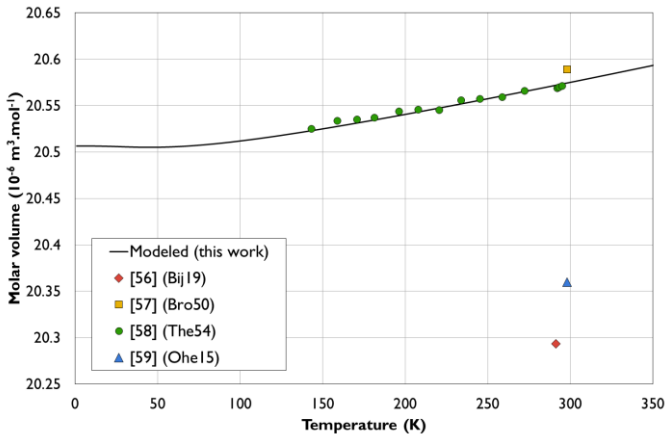

Fig. 4. Experimental and assessed molar volume of α-Sn

3.3 Assessment of β-Sn

The β-Sn phase is stable from 286.35 K to its melting point of 505.078 K [33] at atmospheric pressure. It is commonly referred to as white tin. β-Sn crystallizes in a body-centered tetragonal structure (space group $I4_1/amd$, Pearson symbol *tI*4).

The isobaric heat capacity of β-Sn was recently assessed by Khvan et al. [33]. As for the α-Sn phase, two Einstein frequencies were considered by the authors, and their description is compared with the available data on a supplementary file [54]. It is noted that below the critical temperature of 3.71 K from which β-Sn is a superconductor, the present review does not corroborate the conclusions made by Khvan et al. [33]. A discussion on the matter is provided in the supplementary file mentioned above. Nonetheless, as this discrepancy was only obtained in the extremely low temperature range, its impact on the overall quality of the fit proposed by the authors is largely negligible. At higher temperatures and over the range

relevant to determine the parameters of interest for this work, the description provided by Khvan et al. [33] is very robust, and is therefore accepted in the present study.

The experimental data relative to the molar volume [59,72–82], thermal expansion coefficient [79,83–92], and bulk modulus [93,75,84,94–99] of β-Sn are reviewed in Table 2. Several clarifications are given as follows regarding the treatment of those data. First, regarding the dataset from Balzer et al. [79], measurements along the a-axis and the c-axis were not performed at the same temperatures. Therefore, the data had to be fitted using quadratic polynomials in order to obtain the volumetric thermal expansion coefficient and the molar volume. Second, the thermal expansion coefficient data tabulated by Deshpande et al. [76,77] were obtained by a graphical fit from their x-ray diffraction measurements, as detailed in another work [100]. Some significantly different parameters were obtained when performing a numerical fit of the authors' data. In the present study, only their original molar volume measurements will be considered. Third, the data from Childs and Weintroub [88] were re-calculated including the new measurements from Vernon and Weintroub [89] according to the authors' method. Besides, the data points from Bridgman [94] were extrapolated from higher pressure measurements. Next, the bulk modulus was calculated from the available elastic constants data [93,75,95–99] using the Voigt-Reuss-Hill approximation as detailed in the appendix. Finally, the adiabatic bulk modulus data were converted into isothermal data according to Eq. (18) using the isobaric heat capacity function modeled by Khvan et al. [33] and the results from a preliminary fit of the molar volume and thermal expansion coefficient.

Table 2 - Experimental data relative to the molar volume, thermal expansion coefficient and bulk modulus of β-Sn at atmospheric pressure

Ref	Data	Method	T-range (K)	Relative uncertainty
[72] Jet33	Molar volume	X-ray diffraction (powder)	298.15	1.6%
[73] Str49		X-ray diffraction (N/A)	298.15	0.3%
[74] Lee54		X-ray diffraction (filings)	282 - 455	0.3%
[75] Ray60		X-ray diffraction (single crystal)	4 - 300	N/A
[76] Des61		X-ray diffraction (filings)	308 - 424	0.5%
[77] Des62		X-ray diffraction (filings)	306 - 485	0.4%
[78] Hel64		X-ray diffraction (powder)	298.15	N/A
[79] Bal79		X-ray diffraction (single crystal)	300 - 496	0.01%
[80] Oli84		X-ray diffraction (powder)	300	N/A
[81] Liu86		X-ray diffraction (powder)	298.15	0.2%
[59] Oeh15		X-ray diffraction (nanoparticles)	298.15	N/A
[82] All16		Neutron powder diffraction	298	N/A
[83] Dor07	Thermal expansion	Interferometric dilatometer (cast)	103 - 283	0.1%
[84] Bri25		Dilatometry (single crystal)	298.15	N/A
[85] Shi33		X-ray diffraction (powder)	387	N/A
[86] Gru34		Dilatometry	303 - 473	N/A
[87] Erf39		Interferometric dilatometer (single crystal)	68 - 283	N/A
[88-89] Chi50&Ver53		Interferometric dilatometer (single crystal)	303 - 493	1 – 5 %
[90] Whi64		Sensitive capacitance technique	4 - 283	N/A
[91] Bal71		Dilatometry	~348	N/A
[92] Cur74		X-ray diffraction (single crystal)		
[79] Bal79		Interferometric dilatometer (single crystal)	300 - 490	N/A
[94] Bri23	Isothermal bulk modulus	Lever apparatus (Cast & extruded rod)	303 - 348	N/A
[84] Bri25		Lever apparatus (single crystal)	298.15	30%

[95] Pra55	Isothermal elastic constants	Diffuse x-ray reflection method (single crystal)	298.15	7%
[96] Mas56	Adiabatic elastic constants	Ultrasonic method (single crystal)	298.15	N/A
[97] Hou60		Vibratory method	93 - 468	2 – 4.4%
[75] Ray60		Ultrasonic method (single crystal)	4 - 300	N/A
[98] Car63		Ultrasonic method (single crystal)	298.15	1%
[93] Kra72		Ultrasonic method (single crystal)	301 - 505	1 – 3%
[99] Du17		Ultrasonic method combined with Electron backscatter diffraction (EBSD) (polycrystal)	298.15	N/A

The modeled bulk modulus of β-Sn is presented along with experimental data in Fig. 5. Only the datasets from Rayne et al. [75], Cardinal [98], Kramer et al. [93] and Du et al. [99] were considered in the modeling. Justifications for this choice are provided as follows. To begin with, regarding the data extrapolated from high pressure measurements from Bridgman [94], a significant variation was obtained depending on the method of elaboration of the samples, leading to a dispersion of roughly 7% in the results. The obtained values largely include the selected datasets [75,93,98,99]. Then, regarding the latter study from Bridgman [84], the author pointed out that his results were somewhat uncertain and assigned to his data an uncertainty of about ±30%. This measurement was therefore not taken into account, although it is noted an excellent agreement was obtained with the selected datasets [75,93,98,99]. Besides, Prasad and Wooster [95] also attributed a rather high uncertainty to their result, and the calculated bulk modulus was not used in the modeling. Next, regarding the data from Mason et al. [96], Rayne et al. [75] noted that the value for the elastic constants C_{66}, C_{12} and C_{13} obtained by the authors differed significantly from the their own results. No reason could

be advanced by Rayne et al. [75] to explain this discrepancy. This observation can also be extended for other datasets, and the results from Mason et al. [96] were therefore not taken into account in the modeling. Finally, regarding the measurements from House et al. [97], a sudden change in the obtained trend is noted from roughly 200 K, as highlighted in Fig. 5. The fact the bulk modulus measured by the authors [97] increases with increasing temperature is abnormal, and this dataset was therefore not taken into account in the modeling. A satisfying agreement was obtained between the fit and the selected datasets [75,93,98,99].

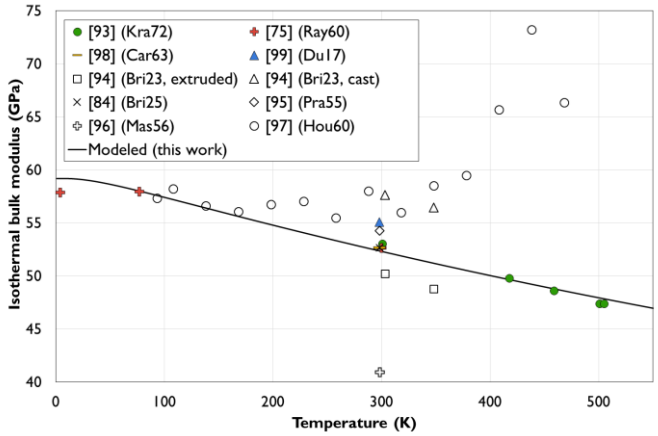

Fig. 5. Experimental and assessed isothermal bulk modulus of β-Sn. The solid symbols represent the data selected in the modeling.

Next, the molar volume and coefficient of thermal expansion of β-Sn were assessed together in a joint optimization based on Eq. (17) and (13). The results are presented along with experimental data in Fig. 6. Regarding the thermal expansion coefficient, the older dataset from Dorsey [83] and the value obtained from the treatment of X-ray diffraction data by Shinoda [85] are clear outliners and were not included in the modeling. Regarding the molar

volume data, a scatter of roughly 0.7% is observed on the measurements made at room temperature. The measurements from Olijnyx et al. [80] and Oehl [59] are consistent and represent the upper limit, whereas the data from Jette [72], Straumanis [73], Lee et al. [74] and Balzer et al. [79] are also consistent and represent the lower limit. In this work, the dataset in the middle containing the consistent measurements of 6 different authors [75–78,81,82] was selected. To select one of the three global trend was preferred, as it is argued that using a mean value for all measurements was more arbitrary. Nevertheless, the temperature dependence of the molar volume as measured by Lee et al. [74] and Balzer et al. [79] was taken into account by shifting the original data to the selected value at 298 K. It is underlined that although two Einstein modes of vibration are considered in the description, only a single global Grüneisen parameter was used, as it was sufficient to obtain a satisfying fit of the data in view of their scattering.

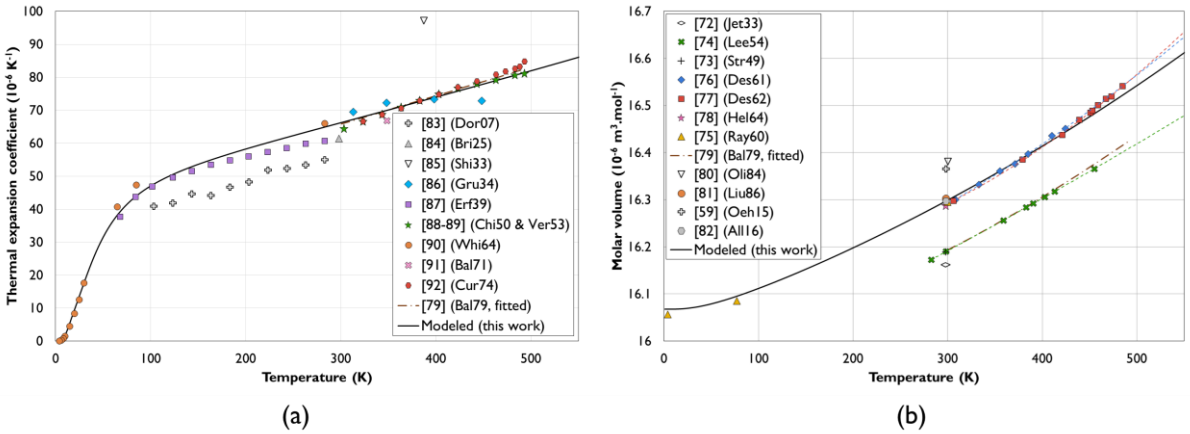

Fig. 6. Experimental and assessed (a) thermal expansion coefficient and (b) molar volume of β-Sn. The solid symbols represent the data selected in the modeling. In (b), the dashed lines are quadratic polynomial fits of the molar volume data from Deshpande et al. [76,77] and Lee et al. [74] plotted to guide the eye.

As the present description is valid down to 0 K, a direct comparison with *ab initio* calculations is possible. Results from Density Functional Theory (DFT) calculations from various studies [101–105] are compared with the present assessment in Table 3. It can be seen that a good agreement was obtained in term of molar volume with the data from Aguado [103] and Yu et al. [104]. However, in term of bulk modulus, both those calculations lead to significantly lower values compared to the present assessment, and a much better agreement is obtained with the data from Cheong and Chang [101].

Table 3 - Comparison between the molar volume and bulk modulus at 0 K obtained in the present description and in the literature by DFT calculations

Ref	Method	V_m (10^{-6} $m^3.mol^{-1}$)	K_T (GPa)
This work	Modeling	16.07	59.20
[104] Yu06	DFT – GGA	15.99 (-0.5%)	52.2 (-11.8%)
[103] Agu03	DFT – LDA	15.89 (-1.1%)	55.3 (-6.6%)
[101] Che91	DFT – LDA	15.20 (-5.4%)	60.5 (+2.2%)
[105] Cui08	DFT – GGA	15.03 (-6.5%)	66.4 (+12.2%)
[102] Cor91	DFT – LDA	14.93 (-7.1%)	63.7 (+7.6%)

3.4 Assessment of solid CaO

Solid CaO is stable up to 3222 K at atmospheric pressure [35], and crystallizes in an NaCl-like face-centered structure (space group $Fm\bar{3}m$, Pearson symbol *cF*8). It is specified here that the aim of the present sub-section is more to put to the test the proposed model and highlight some of its features than to provide a thorough assessment of the thermophysical properties of CaO.

The isobaric heat capacity of solid CaO was recently assessed by Deffrennes et al. [35] using a 3 frequency multi-Einstein model. The authors' description is reviewed along with literature data on a supplementary file attached with the present article [54]. A discussion on the data selection was provided by Deffrennes et al. [35]. The authors' description is supported by both experimental and *ab initio* heat capacity and heat content data, and is accepted in the present

study. The characteristic Einstein temperatures and their corresponding pre-factor will therefore be taken from their work.

The data relative to the molar volume and the thermal expansion coefficient of CaO were reviewed by Bodryakov [106], and the fit proposed by the author is accepted in the present study. Regarding the bulk modulus of solid CaO, it was noted by Song et al. [107] that only scarce data are available, and the authors suggested that the most precise dataset available was the one proposed by Anderson [29]. The data tabulated up to 1200 K by Anderson [29] will therefore be used in the modeling.

The modeled bulk modulus of solid CaO is presented along with the dataset from Anderson [29] in Fig. 7. The agreement between the fit and the data is satisfying.

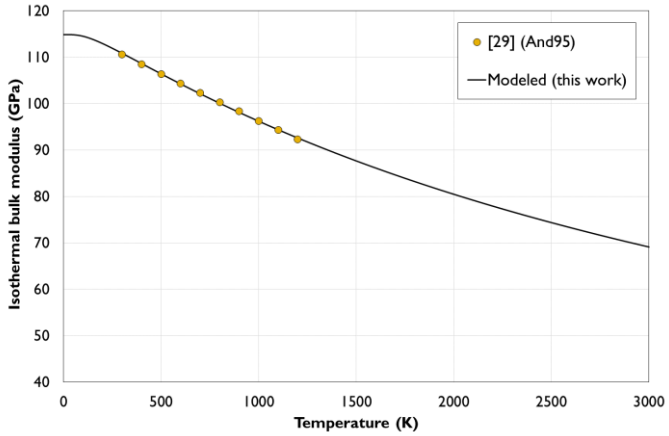

Fig. 7. Experimental and assessed isothermal bulk modulus of CaO

Regarding the thermal expansion coefficient of solid CaO, two different descriptions are provided and compared with the data assessed by Bodryakov [106] in Fig. 8. For both

descriptions, it is noted that the parameter V_{m_0} was optimized so that the value of the molar volume at room temperature of 16.80 10^{-6} $m^3.mol^{-1}$ (8.40 10^{-6} m^3.mol of $atoms^{-1}$) proposed by Bodryakov [106] was perfectly reproduced.

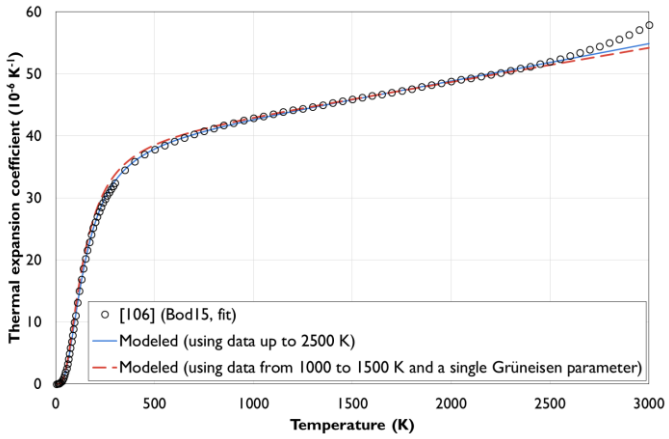

Fig. 8. Experimental thermal expansion coefficient of CaO, and results of two different descriptions. The solid blue line corresponds to the modeling where thermal expansion data were considered up to 2500 K, and where a Grüneisen parameter was optimized for each mode of vibration of the multi-Einstein model. The dashed red line corresponds to the modeling where thermal expansion data were only considered from 1000K to 1500K, and for which a single global Grüneisen parameter was used.

Regarding the first description plotted as a solid blue line in Fig. 8, the aim was to see whether a close fit of the low temperature thermal expansion of a material with a rather high Debye temperature of 673K [29] could be obtained. Indeed, the present model was built based on the hypothesis that the ratio of the Grüneisen parameter over the volume was temperature-independent whatever the temperature, although this approximation is considered to hold only

above the Debye temperature. In this attempt, the tabulated thermal expansion data from Bodryakov [106] were used up to 2500 K to optimize all 3 Grüneisen parameters corresponding to each Einstein vibrational frequency modeled by Deffrennes et al. [35]. A satisfying fit is obtained up to 2500 K, and notably below 600 K where a maximal absolute discrepancy of 0.4 10^{-6} K^{-1} was obtained. The corresponding deviation relative to the thermal expansion coefficient at room temperature is of 1.2%. Above 2500 K, it is noted that the sudden increase in the thermal expansion coefficient considered by Bodryakov [106] could not be closely reproduced, even when using both parameters proposed in Eq. (7) to account for high temperature anharmonic and electronic contributions. To some extent, a consistent trend was proposed for the isobaric heat capacity by Deffrennes et al. [35], and similar difficulties were experienced by the authors as this increase occurs at a very high temperature. Nonetheless, it is important to highlight that the underlying datasets that were used by Bodryakov [106] are highly debated above 1500 K. Besides, none of the original experimental measurements reviewed by the author [106] indicate that the thermal expansion coefficient should increase steeply. Indeed, the reported trends are rather linear and monotonous. In fact, it is noted by Bodryakov [106] that his fit is purely mathematical, and not based on any model or physical consideration. Therefore, it is concluded that the sudden increase above 2500K in the thermal expansion coefficient proposed by the author [106] is too uncertain to assess whether the fact it could not be reproduced here is a limitation of the proposed formalism.

In the proposed model, a self-consistent description of the heat capacity, bulk modulus, thermal expansion coefficient and molar volume is provided using parameters carrying

explicit physical meaning. Therefore, it is expected that reasonable extrapolations can be obtained from it. To investigate on this feature was the aim of the second description proposed here, which is plotted as a dashed red line in Fig. 8. In this second attempt, the fit from Bodryakov [106] was solely used from 1000K to 1500K, and only a single Grüneisen parameter common for all 3 modes of vibrations was considered. Therefore, as the bulk modulus, heat capacity, and molar volume at room temperature are known, there was in practice only three degrees of freedom in the optimization of the parameters (γ_{i_0}, A and B). Ultimately, a satisfying fit of the considered restricted dataset was obtained using only two of those parameters, that are γ_{i_0} and A. Following this procedure, a reliable extrapolation of the lower temperature thermal expansion was obtained, as it can be seen in Fig. 8. Indeed, a maximal absolute discrepancy of 1.6 10^{-6} K^{-1} was obtained, corresponding to a deviation relative to the thermal expansion at room temperature of 4.8%. This is an interesting result, and a promising insight that the present model can lead to reliable extrapolations with scarce data once some of the properties intrinsically linked in the description are known.

3.5 Model parameters

The bulk modulus, thermal expansion coefficient and molar volume that were determined for α-Sn, β-Sn and solid CaO in sections 3.2, 3.3 and 3.4 respectively are presented in Table 4.

Table 4 - Bulk modulus, thermal expansion coefficient and molar volume as determined in this work in the modeling of α-Sn, β-Sn and solid CaO. The reference temperature is taken at 0 K. The properties derived from the given parameters are obtained in the International System of Units (SI).

Description of the parameters used in the multi-Einstein model for each ith mode of vibration							
Phase	a_1	a_2	a_3	θ_1	θ_2	θ_3	Ref
α-Sn	0.67374	0.32626	-	218.4858	61.9652	-	Khv
β-Sn	0.64684	0.35316	-	159.07493	61.12222	-	Khv
CaO	1.142993	0.62542	0.218718	369.447	601.229	188.291	Def

Description of the bulk modulus according to Eq. (11) and (9)		
Phase	χ_{T_0}	C
α-Sn	1.769308E-11	2.896475E-12
β-Sn	1.689306E-11	8.915001E-13
CaO	8.704446E-12	3.863062E-13

Description of the thermal expansion coefficient according to Eq. (16)						
Phase	V_{m_0}	γ_{i_1}	γ_{i_2}	γ_{i_3}	A	B
α-Sn	2.050652E-05	1.620406	-0.7053840	-	-	-
β-Sn	1.606773E-05	1.839411		-	7.649397E-4	-
CaO (assessment)	1.671192E-05	1.257133	2.023413	1.265581	2.764858E-5	-
CaO (demonstrative example)	1.670617E-05	1.517934			1.282848E-5	-
Obtainment of the molar volume using the above parameters according to Eq. (17) and (13)						

Conclusions

In the present study, a semi-empirical model to describe the temperature dependence of the bulk modulus, thermal expansion coefficient, and molar volume was proposed. It is built based on two main cornerstones. The first one is the Grüneisen parameter, which enables to achieve a self-consistent description of all the above properties together with heat capacity. The second one is the multi-frequency Einstein model, which notably enables to achieve direct compatibility with 3rd generation CALPHAD databases. The model parameters carry explicit physical meaning, and the obtained descriptions are valid down to 0K. Plus, compared to isolated descriptions of the heat capacity, bulk modulus, and thermal expansion coefficient using polynomials, it is noted that less parameters may be needed overall.

The proposed model was used in the assessment of α-Sn and β-Sn, for which a critical review of the literature data was provided, and of solid CaO. In this process, several key features of the model were highlighted. First of all, satisfying descriptions of the considered thermophysical properties were obtained while the parameters for the multi-Einstein model were taken directly from 3rd generation CALPHAD assessment of heat capacity data. This is a demonstration of the self-consistency of the model, and of its compatibility with CALPHAD databases. Plus, the present description was proven to be flexible in the sense that the unusual negative thermal expansion coefficient of α-Sn at very low temperature was satisfyingly accounted for. Second, compared to phenomenological polynomial fits used so far, the proposed model enables a direct integration of *ab initio* calculations performed at 0K in the analysis, as it was highlighted in the case of β-Sn. Besides, to build the model, the hypothesis

that the ratio of the Grüneisen parameter over the volume was temperature-independent whatever the temperature was made. It may be a limitation of the model below the Debye temperature. Nonetheless, it was highlighted for all materials considered in this study, and notably in the case of CaO which have a relatively high Debye temperature, that a satisfying description could be obtained in this temperature range. Finally, the present description has the potential to lead to reliable extrapolations when performing a joint analysis of heat capacity, bulk modulus, thermal expansion coefficient and molar volume data. This benefit was highlighted in the CaO case study.

A key strength of the CALPHAD method is that the description of a system is provided based on a consistent assessment of both thermodynamic and phase equilibria data. By this process, the obtained modeling is more reliable. The present model may provide a tool to extend this consistency to the molar volume and related properties. Indeed, thermal expansion data may for instance be used to critically assess debated heat capacity measurements, or to provide reliable extrapolations out of scarce data. Besides, the present work may be interesting in the perspective of building Gibbs energy databases valid up to high pressures. Indeed, it was suggested by Lu and Chen [27] that inconsistent results were obtained so far due to the fact that the heat capacity, thermal expansion and bulk modulus at atmospheric pressure were assessed separately using polynomials which do not hold any physical meaning, causing their intrinsic relations to be lost. In this study, an attempt to capture this intrinsic relationship is provided. It may therefore be a step towards the establishment of high pressure Gibbs energy databases. Finally, as the proposed model is compatible with the CALPHAD framework, it

can be used to develop multi-component molar volume databases as a part of the ICME approach. With this aim in mind, to further investigate the composition dependence of the molar volume and related properties as well as the 3rd generation CALPHAD modeling of solution phases are important perspectives for the future.

Acknowledgements and data statement

This research did not receive any specific grant from funding agencies in the public, commercial, or not-for-profit sectors. Fruitful exchange within the French consortium in high temperature thermodynamics GDR CNRS n°3584 (TherMatHT) are acknowledged.

All the data reviewed in this work and the result of the present modeling, including the databases files, are associated in an open access Mendeley Data repository [54].

Appendix - Computation of the bulk modulus from the elastic constants in the Voigt-Reuss-Hill approximation

The bulk modulus is calculated from the stiffness tensor by the Voigt approximation, according to:

$$K_V = \frac{c_{11} + c_{22} + c_{33} + 2(c_{12} + c_{23} + c_{13})}{9} \quad (A.1)$$

with c_{ij} the elastic constants. Using the Reuss approximation, the bulk modulus is obtained from the compliance tensor such as:

$$\frac{1}{K_R} = s_{11} + s_{22} + s_{33} + 2(s_{12} + s_{23} + s_{13}) \quad (A.2)$$

Using Voigt and Reuss approximation, an upper and lower bond for the bulk modulus are respectively obtained. In the Voigt-Reuss-Hill approximation, the bulk modulus is finally calculated as:

$$K_{VRH} = \frac{K_V + K_R}{2} \quad (A.3)$$

References

[1] G. Isgrò, C.J. Kleverlaan, H. Wang, A.J. Feilzer, Thermal dimensional behavior of dental ceramics, Biomaterials. 25 (2004) 2447–2453. https://doi.org/10.1016/j.biomaterials.2003.09.027.

[2] Y.F. Fu, Y.L. Wong, C.A. Tang, C.S. Poon, Thermal induced stress and associated cracking in cement-based composite at elevated temperatures—Part I: Thermal cracking around single inclusion, Cement and Concrete Composites. 26 (2004) 99–111. https://doi.org/10.1016/S0958-9465(03)00086-6.

[3] M. Martena, D. Botto, P. Fino, S. Sabbadini, M.M. Gola, C. Badini, Modelling of TBC system failure: Stress distribution as a function of TGO thickness and thermal expansion mismatch, Engineering Failure Analysis. 13 (2006) 409–426. https://doi.org/10.1016/j.engfailanal.2004.12.027.

[4] F. Jardine, Thermal Expansion in Automotive-Engine Design, in: 1930: p. 300010. https://doi.org/10.4271/300010.

[5] Y.-L. Shen, A. Needleman, S. Suresh, Coefficients of thermal expansion of metal-matrix composites for electronic packaging, MMTA. 25 (1994) 839–850. https://doi.org/10.1007/BF02665460.

[6] K. Enya, N. Yamada, T. Imai, Y. Tange, H. Kaneda, H. Katayama, M. Kotani, K. Maruyama, M. Naitoh, T. Nakagawa, T. Onaka, M. Suganuma, T. Ozaki, M. Kume, M.R. Krödel, High-precision CTE measurement of hybrid C/SiC composite for cryogenic space telescopes, Cryogenics. 52 (2012) 86–89. https://doi.org/10.1016/j.cryogenics.2011.10.004.

[7] B. Korojy, Volume Change Effects during Solidification of Alloys, Royal Institute of Technology (KTH), 2009.

[8] G.B. Olson, Preface to the viewpoint set on: The Materials Genome, Scripta Materialia. 70 (2014) 1–2. https://doi.org/10.1016/j.scriptamat.2013.09.013.

[9] L. Kaufman, J. Ågren, CALPHAD, first and second generation – Birth of the materials genome, Scripta Materialia. 70 (2014) 3–6. https://doi.org/10.1016/j.scriptamat.2012.12.003.

[10] Y. Du, B. Sundman, Thermophysical Properties: Key Input for ICME and MG, J. Phase Equilib. Diffus. 38 (2017) 601–602. https://doi.org/10.1007/s11669-017-0527-x.

[11] K. Wang, R.R. Reeber, The role of defects on thermophysical properties: Thermal expansion of V, Nb, Ta, Mo and W, Materials Science and Engineering: R: Reports. 23 (1998) 101–137. https://doi.org/10.1016/S0927-796X(98)00011-4.

[12] X. Lu, M. Selleby, B. Sundman, Theoretical modeling of molar volume and thermal expansion, Acta Materialia. 53 (2005) 2259–2272. https://doi.org/10.1016/j.actamat.2005.01.049.

[13] A.F. Guillermet, Critical evaluation of the thermodynamic properties of cobalt, Int J Thermophys. 8 (1987) 481–510. https://doi.org/10.1007/BF00567107.

[14] S.K. Saxena, N. Chatterjee, Y. Fei, G. Shen, Thermodynamic Data on Oxides and Silicates, Springer Berlin Heidelberg, Berlin, Heidelberg, 1993. https://doi.org/10.1007/978-3-642-78332-6.
[15] L.E. Fried, W.M. Howard, Explicit Gibbs free energy equation of state applied to the carbon phase diagram, Phys. Rev. B. 61 (2000) 8734–8743. https://doi.org/10.1103/PhysRevB.61.8734.
[16] M.H.G. Jacobs, H.A.J. Oonk, A new equation of state based on Grover, Getting and Kennedy's empirical relation between volume and bulk modulus. The high-pressure thermodynamics of MgO, Phys. Chem. Chem. Phys. 2 (2000) 2641–2646. https://doi.org/10.1039/a910247g.
[17] O.B. Fabrichnaya, S.K. Saxena, P. Richet, E.F. Westrum, Thermodynamic Data, Models, and Phase Diagrams in Multicomponent Oxide Systems: An Assessment for Materials and Planetary Scientists Based on Calorimetric, Volumetric and Phase Equilibrium Data, Springer Berlin Heidelberg, Berlin, Heidelberg, 2004. https://doi.org/10.1007/978-3-662-10504-7.
[18] X.-G. Lu, M. Selleby, B. Sundman, Implementation of a new model for pressure dependence of condensed phases in Thermo-Calc, Calphad. 29 (2005) 49–55. https://doi.org/10.1016/j.calphad.2005.04.001.
[19] E. Brosh, G. Makov, R.Z. Shneck, Application of CALPHAD to high pressures, Calphad. 31 (2007) 173–185. https://doi.org/10.1016/j.calphad.2006.12.008.
[20] A.S. Piazzoni, G. Steinle-Neumann, H.-P. Bunge, D. Dolejš, A mineralogical model for density and elasticity of the Earth's mantle: MANTLE MINERALOGY AND PHYSICS, Geochem. Geophys. Geosyst. 8 (2007) n/a-n/a. https://doi.org/10.1029/2007GC001697.
[21] T. Komabayashi, Y. Fei, Internally consistent thermodynamic database for iron to the Earth's core conditions, J. Geophys. Res. 115 (2010) B03202. https://doi.org/10.1029/2009JB006442.
[22] T.J.B. Holland, R. Powell, An improved and extended internally consistent thermodynamic dataset for phases of petrological interest, involving a new equation of state for solids: THERMODYNAMIC DATASET FOR PHASES OF PETROLOGICAL INTEREST, Journal of Metamorphic Geology. 29 (2011) 333–383. https://doi.org/10.1111/j.1525-1314.2010.00923.x.
[23] J.C. Jie, C.M. Zou, E. Brosh, H.W. Wang, Z.J. Wei, T.J. Li, Microstructure and mechanical properties of an Al–Mg alloy solidified under high pressures, Journal of Alloys and Compounds. 578 (2013) 394–404. https://doi.org/10.1016/j.jallcom.2013.04.184.
[24] X. Liu, K. Oikawa, Assessment of the temperature and pressure dependence of molar volume and phase diagrams of Cu and Zn, Calphad. 47 (2014) 114–122. https://doi.org/10.1016/j.calphad.2014.07.003.
[25] T.C. Chust, G. Steinle-Neumann, D. Dolejš, B.S.A. Schuberth, H.-P. Bunge, MMA-EoS: A Computational Framework for Mineralogical Thermodynamics: MMA-EOS MINERALOGIC THERMODYNAMICS FRAMEWORK, J. Geophys. Res. Solid Earth. 122 (2017) 9881–9920. https://doi.org/10.1002/2017JB014501.

[26] T. Hammerschmidt, I.A. Abrikosov, D. Alfè, S.G. Fries, L. Höglund, M.H.G. Jacobs, J. Koßmann, X.-G. Lu, G. Paul, Including the effects of pressure and stress in thermodynamic functions: Pressure and stress in thermodynamic functions, Phys. Status Solidi B. 251 (2014) 81–96. https://doi.org/10.1002/pssb.201350156.
[27] X.-G. Lu, Q. Chen, A CALPHAD Helmholtz energy approach to calculate thermodynamic and thermophysical properties of fcc Cu, Philosophical Magazine. 89 (2009) 2167–2194. https://doi.org/10.1080/14786430903059004.
[28] Y.-L. He, X.-G. Lu, N.-Q. Zhu, B. Sundman, CALPHAD modeling of molar volume, Chin. Sci. Bull. 59 (2014) 1646–1651. https://doi.org/10.1007/s11434-014-0218-5.
[29] O.L. Anderson, Equations of state of solids for geophysics and ceramic science, Oxford University Press, New York, 1995.
[30] B. Hallstedt, N. Dupin, M. Hillert, L. Höglund, H.L. Lukas, J.C. Schuster, N. Solak, Thermodynamic models for crystalline phases. Composition dependent models for volume, bulk modulus and thermal expansion, Calphad. 31 (2007) 28–37. https://doi.org/10.1016/j.calphad.2006.02.008.
[31] S. Bigdeli, H. Mao, M. Selleby, On the third-generation Calphad databases: An updated description of Mn: On the third-generation Calphad databases, Phys. Status Solidi B. 252 (2015) 2199–2208. https://doi.org/10.1002/pssb.201552203.
[32] S. Bigdeli, Q. Chen, M. Selleby, A New Description of Pure C in Developing the Third Generation of Calphad Databases, J. Phase Equilib. Diffus. 39 (2018) 832–840. https://doi.org/10.1007/s11669-018-0679-3.
[33] A.V. Khvan, T. Babkina, A.T. Dinsdale, I.A. Uspenskaya, I.V. Fartushna, A.I. Druzhinina, A.B. Syzdykova, M.P. Belov, I.A. Abrikosov, Thermodynamic properties of tin: Part I Experimental investigation, ab-initio modelling of α-, β-phase and a thermodynamic description for pure metal in solid and liquid state from 0 K, Calphad. 65 (2019) 50–72. https://doi.org/10.1016/j.calphad.2019.02.003.
[34] A. Dinsdale, O. Zobac, A. Kroupa, A. Khvan, Use of third generation data for the elements to model the thermodynamics of binary alloy systems: Part 1 – The critical assessment of data for the Al-Zn system, Calphad. 68 (2020) 101723. https://doi.org/10.1016/j.calphad.2019.101723.
[35] G. Deffrennes, N. Jakse, C.M.S. Alvares, I. Nuta, A. Pasturel, A. Khvan, A. Pisch, Thermodynamic modelling of the Ca–O system including 3rd generation description of CaO and CaO2, Calphad. 69 (2020) 101764. https://doi.org/10.1016/j.calphad.2020.101764.
[36] Z. He, B. Kaplan, H. Mao, M. Selleby, The third generation Calphad description of Al–C including revisions of pure Al and C, Calphad. 72 (2021) 102250. https://doi.org/10.1016/j.calphad.2021.102250.
[37] X.-G. Lu, M. Selleby, B. Sundman, Assessments of molar volume and thermal expansion for selected bcc, fcc and hcp metallic elements, Calphad. 29 (2005) 68–89. https://doi.org/10.1016/j.calphad.2005.05.001.
[38] B. Hallstedt, Molar volumes of Al, Li, Mg and Si, Calphad. 31 (2007) 292–302. https://doi.org/10.1016/j.calphad.2006.10.006.

[39] B. Zhang, X. Li, D. Li, Assessment of thermal expansion coefficient for pure metals, Calphad. 43 (2013) 7–17. https://doi.org/10.1016/j.calphad.2013.08.006.
[40] J.-P. Poirier, Introduction to the Physics of the Earth's Interior, 2nd ed., Cambridge University Press, 2000. https://doi.org/10.1017/CBO9781139164467.
[41] M.W. Chase, I. Ansara, A. Dinsdale, G. Eriksson, G. Grimvall, L. Höglund, H. Yokokawa, Workshop on thermodynamic models and data for pure elements and other endmembers of solutions, Calphad. 19 (1995) 437–447. https://doi.org/10.1016/0364-5916(96)00002-8.
[42] A.R. Oganov, P.I. Dorogokupets, Intrinsic anharmonicity in equations of state and thermodynamics of solids, J. Phys.: Condens. Matter. 16 (2004) 1351–1360. https://doi.org/10.1088/0953-8984/16/8/018.
[43] P.I. Dorogokupets, A.M. Dymshits, K.D. Litasov, T.S. Sokolova, Thermodynamics and Equations of State of Iron to 350 GPa and 6000 K, Sci Rep. 7 (2017) 41863. https://doi.org/10.1038/srep41863.
[44] M.H.G. Jacobs, R. Schmid-Fetzer, Thermodynamic properties and equation of state of fcc aluminum and bcc iron, derived from a lattice vibrational method, Phys Chem Minerals. 37 (2010) 721–739. https://doi.org/10.1007/s00269-010-0371-6.
[45] Z. Lin, L.V. Zhigilei, V. Celli, Electron-phonon coupling and electron heat capacity of metals under conditions of strong electron-phonon nonequilibrium, Phys. Rev. B. 77 (2008) 075133. https://doi.org/10.1103/PhysRevB.77.075133.
[46] T. Tsuchiya, K. Kawamura, First-principles electronic thermal pressure of metal Au and Pt, Phys. Rev. B. 66 (2002) 094115. https://doi.org/10.1103/PhysRevB.66.094115.
[47] Y.P. Varshni, Temperature Dependence of the Elastic Constants, Phys. Rev. B. 2 (1970) 3952–3958. https://doi.org/10.1103/PhysRevB.2.3952.
[48] H. Ledbetter, Relationship between Bulk-Modulus Temperature Dependence and Thermal Expansivity, phys. stat. sol. (b). 181 (1994) 81–85. https://doi.org/10.1002/pssb.2221810109.
[49] A.F. Guillermet, Trita-Mac-0325, Royal Institute of Technology, Sweden. (1987).
[50] W.-H. Xiong, W. Liu, M.-M. Dai, J.-Q. Liu, X.-G. Lu, Assessments of molar volumes of Co-, Ni- and Ti- related bcc and fcc phases, Calphad. 66 (2019) 101629. https://doi.org/10.1016/j.calphad.2019.101629.
[51] D. Huang, S. Liu, Y. Du, B. Sundman, Modeling of the molar volume of the solution phases in the Al–Cu–Mg system, Calphad. 51 (2015) 261–271. https://doi.org/10.1016/j.calphad.2015.10.006.
[52] J. Schmitz, B. Hallstedt, J. Brillo, I. Egry, M. Schick, Density and thermal expansion of liquid Al–Si alloys, J Mater Sci. 47 (2012) 3706–3712. https://doi.org/10.1007/s10853-011-6219-8.
[53] J.-O. Andersson, T. Helander, L. Höglund, P. Shi, B. Sundman, Thermo-Calc & DICTRA, computational tools for materials science, Calphad. 26 (2002) 273–312. https://doi.org/10.1016/S0364-5916(02)00037-8.
[54] G. Deffrennes, B. Oudot, Data for: A self-consistent model to describe the temperature dependence of the bulk modulus, thermal expansion and molar volume compatible with

3rd generation CALPHAD databases, Mendeley Data, V1. (n.d.). http://dx.doi.org/10.17632/xskt8cj82b.1.
[55] 2008 TCC Thermo-Calc Software User's Guide Version S. Available online: https://thermocalc.com/support/documentation/, (2008).
[56] A.J. Bijl, N.H. Kolkmeijer, Investigation by means of X-rays of the crystal structure of white and grey tin. III. The structure of grey tin, Proc. Roy. Acad. Sci. Amsterdam. 21 (1919) 501–504.
[57] L.D. Brownlee, Lattice Constant of Grey Tin, Nature. 166 (1950) 482–482. https://doi.org/10.1038/166482a0.
[58] J. Thewlis, A.R. Davey, Thermal Expansion of Grey Tin, Nature. 174 (1954) 1011–1011. https://doi.org/10.1038/1741011a0.
[59] N. Oehl, G. Schmuelling, M. Knipper, R. Kloepsch, T. Placke, J. Kolny-Olesiak, T. Plaggenborg, M. Winter, J. Parisi, In situ X-ray diffraction study on the formation of α-Sn in nanocrystalline Sn-based electrodes for lithium-ion batteries, CrystEngComm. 17 (2015) 8500–8504. https://doi.org/10.1039/C5CE01841B.
[60] S.I. Novikova, Study of the thermal expansion of alpha-Sn, InSb, and CdTe, Soviet Physics, Solid State. 2 (1960) 2087–2089.
[61] P.J. Reddy, S.V. Subrahmanyam, Dependence on Temperature of Elastic Moduli of Tin, Nature. 185 (1960) 29–29. https://doi.org/10.1038/185029a0.
[62] D.L. Price, J.M. Rowe, The crystal dynamics of grey (α) tin at 90°K, Solid State Communications. 7 (1969) 1433–1438. https://doi.org/10.1016/0038-1098(69)90318-4.
[63] C.J. Buchenauer, M. Cardona, F.H. Pollak, Raman Scattering in Gray Tin, Phys. Rev. B. 3 (1971) 1243–1244. https://doi.org/10.1103/PhysRevB.3.1243.
[64] D.L. Price, J.M. Rowe, R.M. Nicklow, Lattice Dynamics of Grey Tin and Indium Antimonide, Phys. Rev. B. 3 (1971) 1268–1279. https://doi.org/10.1103/PhysRevB.3.1268.
[65] R. Hill, The Elastic Behaviour of a Crystalline Aggregate, Proc. Phys. Soc. A. 65 (1952) 349–354. https://doi.org/10.1088/0370-1298/65/5/307.
[66] D.-H. Chung, Elastic moduli of single crystal and polycrystalline MgO, Philosophical Magazine. 8 (1963) 833–841. https://doi.org/10.1080/14786436308213840.
[67] G.R. Barsch, Adiabatic, Isothermal, and Intermediate Pressure Derivatives of the Elastic Constants for Cubic Symmetry. I. Basic Formulae, phys. stat. sol. (b). 19 (1967) 129–138. https://doi.org/10.1002/pssb.19670190115.
[68] J. Ihm, M.L. Cohen, Equilibrium properties and the phase transition of grey and white tin, Phys. Rev. B. 23 (1981) 1576–1579. https://doi.org/10.1103/PhysRevB.23.1576.
[69] C.O. Rodríguez, V.A. Kuz, E.L. Peltzer y Blancá, O.M. Cappannini, Structural properties of tetrahedrally coordinated crystals from first-principles calculations of pressure and total energies, Phys. Rev. B. 31 (1985) 5327–5334. https://doi.org/10.1103/PhysRevB.31.5327.
[70] I. Ishida, Negative Thermal Expansion Coefficient of Diamond Structure Crystal, J. Phys. Soc. Jpn. 39 (1975) 1282–1291. https://doi.org/10.1143/JPSJ.39.1282.
[71] R.W.G. Wyckoff, Crystal Structures, Second edition, Interscience Publishers, New York, New York, 1963.

[72] E.R. Jette, E.B. Gebert, An X-Ray Study of the Binary Alloys of Silicon with Ag, Au, Pb, Sn, Zn, Cd, Sb and Bi, The Journal of Chemical Physics. 1 (1933) 753–755. https://doi.org/10.1063/1.1749242.
[73] M.E. Straumanis, The Precision Determination of Lattice Constants by the Powder and Rotating Crystal Methods and Applications, Journal of Applied Physics. 20 (1949) 726–734. https://doi.org/10.1063/1.1698520.
[74] J.A. Lee, G.V. Raynor, The Lattice Spacings of Binary Tin-Rich Alloys, Proc. Phys. Soc. B. 67 (1954) 737–747. https://doi.org/10.1088/0370-1301/67/10/301.
[75] J.A. Rayne, B.S. Chandrasekhar, Elastic Constants of β Tin from 4.2°K to 300°K, Phys. Rev. 120 (1960) 1658–1663. https://doi.org/10.1103/PhysRev.120.1658.
[76] V.T. Deshpande, D.B. Sirdeshmukh, Thermal expansion of tetragonal tin, Acta Cryst. 14 (1961) 355–356. https://doi.org/10.1107/S0365110X61001212.
[77] V.T. Deshpande, D.B. Sirdeshmukh, Thermal expansion of tin in the β–γ transition region, Acta Cryst. 15 (1962) 294–295. https://doi.org/10.1107/S0365110X62000742.
[78] W.J. Helfrich, R.A. Dodd, Densities and lattice parameters of tin (indium) solid solutions, Acta Metallurgica. 12 (1964) 667–669. https://doi.org/10.1016/0001-6160(64)90039-2.
[79] R. Balzer, H. Sigvaldason, Equilibrium vacancy concentration measurements on tin single crystals, Phys. Stat. Sol. (b). 92 (1979) 143–147. https://doi.org/10.1002/pssb.2220920116.
[80] H. Olijnyk, W.B. Holzapfel, PHASE TRANSITIONS IN Si, Ge AND Sn UNDER PRESSURE, J. Phys. Colloques. 45 (1984) C8-153-C8-156. https://doi.org/10.1051/jphyscol:1984828.
[81] M. Liu, L.-G. Lui, Compressions and phase transitions of tin to half a megabar, High Temp. - High Press. 18 (1986) 79–85.
[82] M.C. Allison, M. Avdeev, S. Schmid, S. Liu, T. Söhnel, C.D. Ling, Synthesis, structure and geometrically frustrated magnetism of the layered oxide-stannide compounds Fe(Fe 3−xMnx)Si2Sn7O16, Dalton Trans. 45 (2016) 9689–9694. https://doi.org/10.1039/C6DT01074A.
[83] H.G. Dorsey, Coefficient of Linear Expansion at Low Temperatures, Phys. Rev. (Series I). 25 (1907) 88–102. https://doi.org/10.1103/PhysRevSeriesI.25.88.
[84] P.W. Bridgman, Certain Physical Properties of Single Crystals of Tungsten, Antimony, Bismuth, Tellurium, Cadmium, Zinc, and Tin, Proceedings of the American Academy of Arts and Sciences. 60 (1925) 305. https://doi.org/10.2307/25130058.
[85] G. Shinoda, X-Ray Investigations on the Thermal Expansion of Solids (Part 1), Memoirs of the College of Science, Kyoto Imperial University. Series A. 16 (1933) 193–201.
[86] G. Grube, H. Voßkühler, Elektrische Leitfähigkeit und Zustandsdiagramm bei Binären Legierungen. 13. Mitteilung. Über Mischkristallbildung Im System Magnesium-Zinn, Ztschr. Elektrochem. Bd. 40 (1934) 566–570. https://doi.org/10.1002/bbpc.19340400806.

[87] H.D. Erfling, Studien zur thermischen Ausdehnung fester Stoffe in tiefer Temperatur. II (Cr, β-Mn, Mo, Rh, Be, Graphit, Tl, Zr, Bi, Sb, Sn und Beryll), Ann. Phys. 426 (1939) 136–160. https://doi.org/10.1002/andp.19394260204.
[88] B.G. Childs, S. Weintroub, The Measurement of the Thermal Expansion of Single Crystals of Tin by an Interferometric Method, Proc. Phys. Soc. B. 63 (1950) 267–277. https://doi.org/10.1088/0370-1301/63/4/303.
[89] E.V. Vernon, S. Weintroub, The Measurement of the Thermal Expansion of Single Crystals of Indium and Tin with a Photoelectric Recording Dilatometer, Proc. Phys. Soc. B. 66 (1953) 887–894. https://doi.org/10.1088/0370-1301/66/10/309.
[90] G.K. White, Thermal expansion of anisotropic metals at low temperatures, Physics Letters. 8 (1964) 294–295. https://doi.org/10.1016/S0031-9163(64)80002-0.
[91] L.J. Balasundaram, A.N. Sinha, Thermal Expansion of Lead-Tin and Lead-Cadmium Alloys, Journal of Applied Physics. 42 (1971) 5207–5207. https://doi.org/10.1063/1.1659926.
[92] M.A. Current, Vacancy Concentrations in Zinc and tin, Faculty of Rensselaer polytechnic Institute, 1974.
[93] W. Kramer, J. Nölting, Anomale spezifische Wärmen und fehlordnung der Metalle indium, Zinn, Blei, Zink, Antimon und Aluminium, Acta Metallurgica. 20 (1972) 1353–1359. https://doi.org/10.1016/0001-6160(72)90070-3.
[94] P.W. Bridgman, The Compressibility of Thirty Metals as a Function of Pressure and Temperature, Proceedings of the American Academy of Arts and Sciences. 58 (1923) 165. https://doi.org/10.2307/20025987.
[95] S.C. Prasad, W.A. Wooster, The study of the elastic constants of white tin by diffuse X-ray reflexion, Acta Cryst. 8 (1955) 682–686. https://doi.org/10.1107/S0365110X55002119.
[96] W.P. Mason, H.E. Bömmel, Ultrasonic Attenuation at Low Temperatures for Metals in the Normal and Superconducting States, The Journal of the Acoustical Society of America. 28 (1956) 930–943. https://doi.org/10.1121/1.1908524.
[97] D.G. House, E.V. Vernon, Determination of the elastic moduli of tin single crystals, and their variation with temperature, Br. J. Appl. Phys. 11 (1960) 254–259. https://doi.org/10.1088/0508-3443/11/6/308.
[98] L.C. Cardinal, NRL Problem No: F03-01, Report of NRL Progress, Naval Research Laboratory. (1963) 31.
[99] X. Du, J.-C. Zhao, Facile measurement of single-crystal elastic constants from polycrystalline samples, Npj Comput Mater. 3 (2017) 17. https://doi.org/10.1038/s41524-017-0019-x.
[100] V.T. Deshpande, V.M. Mudholker, On the Evaluation of the Coefficients of Thermal Expansion of Crystals from X-Ray Data, On the Evaluation of the Coefficients of Thermal Expansion of Crystals from X-Ray Data. 35 (1960) 434–436.
[101] B.H. Cheong, K.J. Chang, First-principles study of the structural properties of Sn under pressure, Phys. Rev. B. 44 (1991) 4103–4108. https://doi.org/10.1103/PhysRevB.44.4103.

[102] J.L. Corkill, A. Garca, M.L. Cohen, Theoretical study of high-pressure phases of tin, Phys. Rev. B. 43 (1991) 9251–9254. https://doi.org/10.1103/PhysRevB.43.9251.
[103] A. Aguado, First-principles study of elastic properties and pressure-induced phase transitions of Sn: LDA versus GGA results, Phys. Rev. B. 67 (2003) 212104. https://doi.org/10.1103/PhysRevB.67.212104.
[104] C. Yu, J. Liu, H. Lu, J. Chen, Ab initio calculation of the properties and pressure induced transition of Sn, Solid State Communications. 140 (2006) 538–543. https://doi.org/10.1016/j.ssc.2006.09.026.
[105] S. Cui, L. Cai, W. Feng, H. Hu, C. Wang, Y. Wang, First-principles study of phase transition of tin and lead under high pressure, Phys. Stat. Sol. (b). 245 (2008) 53–57. https://doi.org/10.1002/pssb.200743240.
[106] V.Y. Bodryakov, Specific Heat and Thermal Expansion of Refractory Nonmetal: CaO, Open Science Journal of Modern Physics. 2 (2015) 50–54.
[107] T. Song, X.W. Sun, R.F. Wang, H.W. Lu, J.H. Tian, P. Guo, Effects of pressure and temperature on the isothermal bulk modulus of CaO, Physica B: Condensed Matter. 406 (2011) 293–296. https://doi.org/10.1016/j.physb.2010.10.071.